Ultrafast electron-phonon scattering in semiconductors studied by nondegenerate four-wave mixing

M. Betz, G. Göger, and A. Leitenstorfer
Physik-Department E 11, Technische Universität München, D-85748 Garching, Germany

K. Ortner and C. R. Becker
Physikalisches Institut, Universität Würzburg, D-97074 Würzburg, Germany

G. Böhm
Walter-Schottky-Institut, Technische Universität München, D-85748 Garching, Germany

A. Laubereau
Physik-Department E 11, Technische Universität München, D-85748 Garching, Germany

Nondegenerate four-wave-mixing allows one to monitor the femtosecond relaxation of free carriers in GaAs and CdTe at densities as low as 2×10^{15} cm^{-3}. The energy relaxation time of electrons via LO-phonon emission is determined to be 240 ± 20 fs in GaAs. In more polar CdTe, this time constant is found to be as short as 70 ± 15 fs which is even shorter than the phonon oscillation period of 200 fs. [S0163-1829(99)51840-7]

In the past few years, femtosecond nonlinear spectroscopy of semiconductors has provided new insight in the coherent and incoherent dynamics of electronic excitations.[1] The two most widely employed experimental techniques have been four-wave-mixing (FWM) and differential transmission spectroscopy (DTS). With FWM in both two and three beam geometries a wealth of information about the coherent interband dynamics has been obtained.[2–6] Differential transmission on the other hand is determined by coherent as well as incoherent dynamics. DTS has provided valuable details about the temporal evolution of nonthermal carrier distributions in semiconductors including the quantum kinetic electron-LO-phonon emission in GaAs.[7,8] The sensitivity of this technique is limited by the small transmission changes in the band-to-band continuum of semiconductors at moderate excitation densities and by the large background of the transmitted probe light. Most of the FWM experiments have essentially been *one-color* in that one performs degenerate measurements and tunes the photon energy. The first *two-color* femtosecond FWM experiments were performed by Cundiff *et al.*[9] and Kim *et al.*[10] Both papers obtained information about the excitonic properties of semiconductors while the coherent as well as the incoherent response of the band-to-band continuum remained unresolved due to the limited sensitivity and insufficient time resolution.

In this communication, the first two-color femtosecond FWM measurements high in the absorption continuum of bulk semiconductors are presented. We have developed a FWM technique that combines properties of FWM and DTS experiments and which has–to our knowledge–not been reported previously. The main advantages are as follows: (i) The investigated signal is produced in a phase-matched and background free direction as in the case of standard FWM experiments. (ii) Our technique monitors the incoherent relaxation of nonthermal carrier distributions in bulk semiconductors with a temporal resolution limited only by the pulse durations as in standard pump-probe experiments. The experimental setup takes advantage of a two-color Ti:sapphire-laser[11,12] which produces two independently tunable transform-limited pulse trains with a temporal jitter below 2 fs. Figure 1(a) schematically depicts the applied FWM technique. It consists of a conventional three-beam FWM geometry except for the fact that two beams are derived from one branch of the two-color Ti:Sapphire laser, while the third is delivered by the second branch. When the two pulses with central frequency ω_1 and wave vectors $\vec{k_1}$ and $\vec{k_2}$ arrive at the sample with a delay t_{12} comparable to or shorter than their pulse duration they form a carrier population grating in the sample from which the third beam with central frequency ω_2 can be diffracted over a broad spectral range. In order to achieve a large modulation depth of the population grating our measurements are performed at $t_{12}=0$. The two degenerate pulses with wavevectors $\vec{k_1}$ and $\vec{k_2}$ serve as the pump in the sense of a DTS experiment. The population grating in the sample results in a modulation of the refractive index and the absorption due to the nonlinear response of the semiconductor. This grating is then probed by the third pulse with central frequency ω_2 and wavevector $\vec{k_3}$ after a delay time t_D.
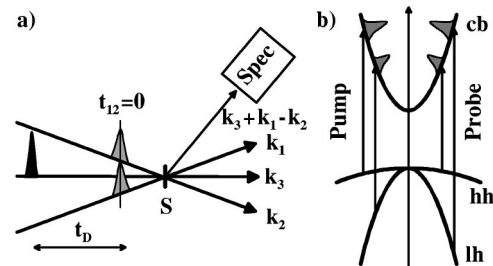
FIG. 1. (a) Scheme of the nondegenerate four-wave-mixing geometry. (b) Schematic band structure and relevant transitions of the investigated semiconductors.
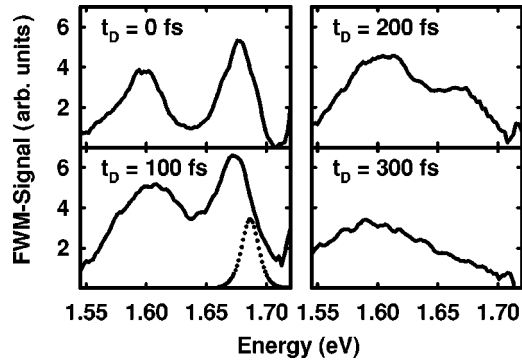
FIG. 2. Spectrally resolved four-wave-mixing signal in GaAs for an average excitation density of 7×10^{15} cm^{-3} for different delay times t_D. The dotted insert at $t_D = 100$ fs shows the excitation spectrum.

The background free signal observed in the phase-matched direction $(\vec{k}_3 + \vec{k}_1 - \vec{k}_2)$ is spectrally resolved and studied as a function of wavelength and delay time t_D.

The third order nonlinear response of the absorption continuum of a semiconductor arises from three different effects: (i) The main nonlinearity at moderate excitation densities is the result of Pauli blocking of band-to-band transitions by photoexcited carriers. As shown in Fig. 1(b) one expects different contributions since both light hole (lh) and heavy hole (hh) transitions are excited by the pump pulses. In addition to the pump frequencies, bleaching effects also occur for other transition energies. As indicated in the right part of Fig. 1(b), electrons generated from the lh band bleach hh transitions with lower energies than the pump energy. Similarly, electrons generated via the hh band lead to a bleaching effect of lh transitions blue-shifted with respect to the pump photon energy. (ii) Coulomb interaction between the generated carriers has been shown to result in a red-shift of the bleaching effect in DTS.[7,8,13] (iii) Collective effects such as band gap renormalization lead to a small background of the signal that is only slowly varying with the photon energy. Therefore the spectrally resolved FWM signal depends strongly on the distribution of the carriers in valence and conduction bands.

At first, experimental data are presented on GaAs. The sample is a bulk GaAs layer of a thickness of 400 nm with AlGaAs cladding and AR-coating on both sides. All experiments are carried out at a temperature of 20 K. The pump pulses with wavevectors $\vec{k}_1$ and $\vec{k}_2$ are tuned to a central photon energy of 1.68 eV and a pulse duration of 90 fs to prepare an energetically narrow initial distribution of carriers in the valence and conduction bands. These two beams are polarized linear and parallel to each other and produce an spatially averaged electron density of 7×10^{15} cm^{-3}. The 20 fs probe pulse with wave vector $\vec{k}_3$ encompasses the entire spectral bandwidth from the excitonic resonance at 1.512 eV to beyond the photon energy of the excitation pulse. The polarization of the probe beam is chosen perpendicular to those of the pump pulses in order to suppress scattered light efficiently via a polarizer and to reduce coherent artifacts. The intensity of the probe pulse is one order of magnitude weaker than that of the pump beams. In Fig. 2 spectrally resolved FWM data are shown for various delay times t_D. The signals depicted here are normalized to the spectral in-
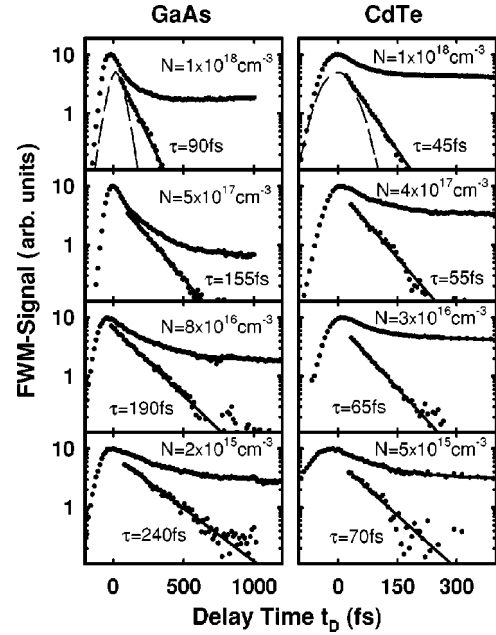
FIG. 3. (a) Four-wave-mixing signal recorded at a photon energy of 1.61 eV for different carrier densities in GaAs (left-hand side). The pump pulse is centered at 1.58 eV. The upper curves display the uncorrected data with a biexponential fit; the lower curves show the signal without the slowly varying background. The average carrier density N and the decay time τ of the rapidly decaying part of the signal are indicated. The additional dashed curve in the top diagram refers to the cross correlation of pump and probe pulse. (b) Analogous measurements for CdTe (right-hand side). Note the different scales of the abscissas.

tensity of the probe pulse at the corresponding photon energy. The main results of these measurements are as follows: For a delay time of $t_D = 0$ fs a signal following the spectral shape of the pump pulse is red-shifted about 10 meV due to Coulomb effects.[7,8,13] The peak at a photon energy of 1.60 eV arises from bleaching of hh transitions by electrons generated from the lh band. After a delay time of $t_D = 100$ fs the minimum between these two components has been reduced by electrons generated from the hh band having emitted one LO-phonon ($\hbar\omega_{LO} = 36$ meV). This relaxation also leads to a broadening of the peak at 1.60 eV. According to the FWM spectra on the right hand side of Fig. 2, the carrier distribution relaxes towards a thermal distribution within several hundreds of femtoseconds as expected from theoretical estimates for the carrier-phonon and carrier-carrier scattering times.

The left part of Fig. 3 shows FWM signals in GaAs taken at a fixed spectral position of 1.61 eV for different carrier densities. In these experiments the pump pulse is centered at 1.58 eV and has a spectral width of 16 meV full width at half maximum and a pulse duration of 100 fs. As a result, the energetic width of the photoexcited carrier distribution in the conduction band is much narrower than the LO-phonon energy of $\hbar\omega_{LO} = 36$ meV. This fact is essential for a quantitative study of LO-phonon emission by electrons since scattering events within the initial distribution are avoided. As indicated in Fig. 1(b) the photogenerated electrons also influence the refractive index and the absorption coefficient at higher photon energies via the bleaching effect of lh transi-
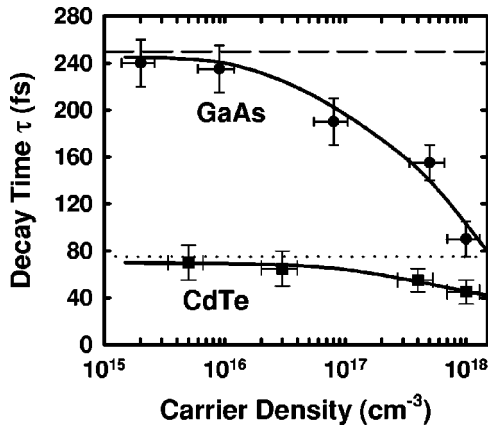
FIG. 4. Decay times τ of the four-wave-mixing signal in GaAs (circles) and CdTe (squares) for different excitation densities. The theoretical LO-emission times via polar optical scattering according to Eq. (1) for electrons in GaAs (dashed line) and CdTe (dotted line) are marked. The solid lines are to guide the eye.

tions by electrons created from hh transitions. Therefore the relaxation of the photo-generated electron distribution can be investigated via transitions at 1.61 eV. This constellation provides two major advantages: (i) Mainly electron dynamics is monitored since the involved lh transitions are not populated by the pump pulse. (ii) Artifacts due to coherent coupling effects between pump and probe pulses are suppressed. The data of Fig. 3 exhibit a biexponential decay with one time constant in the femtosecond regime and a background slowly varying on a time scale of several picoseconds. The faster decay time τ of the signal is as fast as 90 fs for high excitation densities and increases with decreasing carrier density. As depicted in Fig. 4, the relaxation time saturates at 240 ± 20 fs for carrier densities below 1×10^{16} cm^{-3}. These fast decay times can be attributed to the energy relaxation of the photogenerated electrons. For low densities electron-electron scattering is negligible and the time constant of 240 ± 20 fs derived from these FWM data is directly related to the energy relaxation of electrons via LO-phonon emission. For densities above 1×10^{16} cm^{-3} an additional contribution to the energy relaxation via electron-electron scattering becomes significant. It should be noted that the same LO-phonon emission time has recently been determined via ultrasensitive DTS spectroscopy.[7] The previous value agrees perfectly with the present findings. Earlier measurements of the electron-phonon-interaction employed more indirect methods. Kash et al.[14] have investigated the carrier-phonon-interaction via time-resolved Raman spectroscopy. An electron-phonon scattering time of 165 fs was deduced by averaging over 12 emission steps. Levi et al.[15] have derived a scattering time of approximately 180 fs via injected-hot-electron transport. Our measurements provide a more reliable result since we monitor the electronic relaxation directly via the decay time of the FWM signal.

The picosecond component of the signal may be attributed to two mechanisms: (i) Band gap renormalization due to the photoexcited carriers[8] and (ii) the spectral wings of the strong excitonic nonlinearities extending into the band-to-band continuum[10].

We now turn to the results on CdTe. The measurements provide the first experimental investigation of free electron

relaxation in this strongly polar material. The sample consists of a 370 nm bulk CdTe layer. The pump pulse is centered at 1.65 eV with a duration of 100 fs and spectral full width at half maximum of 16 meV. Again, the energetic width of the pump pulse is chosen significantly smaller than $\hbar \omega_{LO} = 21$ meV. The probe pulse is spectrally broad with a pulse duration of 25 fs. According to the right hand side of Fig. 3, the FWM data decay biexponentially. The fast decay time in the femtosecond regime is connected with the energy relaxation of the electrons. As depicted in Fig. 4 the initial decay time increases from a value of 45 fs at a density of 10^{18} cm^{-3} to 70 ± 15 fs for densities below 3×10^{16} cm^{-3}. This finding is closely related to the coupling strength for the LO-phonon emission of the nonequilibrium electrons via the Fröhlich interaction. The polar optical scattering mechanism is of fundamental theoretical interest because the electron-phonon scattering in CdTe should exhibit strong quantum kinetic features. The polaron coupling constant of $\alpha = 0.33$ is relatively large in CdTe as compared to GaAs with $\alpha = 0.06$. The time constant of the scattering process in CdTe is faster than the phonon oscillation period of 200 fs which is generally taken as an estimate for the duration of the interaction process. In Fig. 4, the initial decay times are depicted versus excitation density. The transition to a low density regime where electron-electron interaction is negligible can be seen for both GaAs and CdTe. Of special interest is the observation that the phonon scattering is larger by a factor of three in CdTe compared to GaAs due to the stronger Fröhlich coupling. As a result, the saturation region which is dominated by carrier-lattice interaction extends to higher densities in CdTe.

For the theoretical interpretation of the relaxation times in GaAs and CdTe we assume a pure Fröhlich type electron-phonon interaction.[16] The polar optical scattering dominates the energy transfer to the lattice since deformation potential scattering with optical phonons is forbidden in the Γ-valley of zincblende materials due to symmetry considerations.[17] The scattering rate can be calculated analytically for electrons in a parabolic conduction band via Fermi's golden rule. In first order perturbation theory the scattering rate for an electron with effective mass m_Γ and kinetic energy E_e is given by

$$\Gamma_{e-LO} = \sqrt{\frac{m_\Gamma}{2E_e}} \frac{e^2 \omega_{LO}}{2\pi \hbar \epsilon_0} \left(\frac{1}{\epsilon_\infty} - \frac{1}{\epsilon_s} \right) \text{Arsinh} \left(\sqrt{\frac{E_e}{\hbar \omega_{LO}} - 1} \right) \quad (1)$$

This expression is derived in Ref. 17 and is valid for negligible phonon occupation, i.e. for low temperatures $T \ll \hbar \omega_{LO} / k_B$ and for dispersionless LO-phonons. The relevant material parameters for GaAs and CdTe are given in Table I. In our experiments the average kinetic energies of the electrons initially excited by hh transitions is 65 meV for the measurements in GaAs and 45 meV for those in CdTe. The scattering times calculated from Eq. (1) are 255 fs in GaAs and 75 fs in CdTe in very good agreement with our experimental results. This agreement is surprising especially for the case of strongly polar CdTe considering the simplicity of our estimate: Eq. (1) takes into account only first order perturbation theory. Until now it has not been clarified if this approximation is still sufficient for a polaron coupling con-

TABLE I. Material parameters taken from Ref. 19 for the calculation of the scattering rate of electrons in GaAs and CdTe m_0: free electron mass. ϵ_∞, ϵ_s: dielectric constants in the high frequency and static limit.

	GaAs	CdTe
m_Γ/m_0	0.067	0.090
$\hbar\omega_{LO}$ (meV)	36	21
ϵ_∞	10.9	7.1
ϵ_s	12.5	10.2

stant as large as $\alpha=0.33$ because α is expected to be a measure for the relative importance of higher-order processes. In both materials we do not see evidence for a non-exponential decay of the photogenerated electron distribution which might be expected in a strong coupling regime.[18]

In conclusion we have presented a special application for nondegenerate FWM experiments. The results are not accessible with usual two beam or three beam degenerate FWM techniques. Our method provides a background free alternative for DTS experiments and offers therefore a variety of applications in the investigation of femtosecond dynamics. In the first measurements with this technique we have monitored femtosecond free carrier relaxation in GaAs and CdTe and investigated the electron-LO-phonon interaction at low densities where carrier-carrier scattering is negligible. Our findings are consistent with the assumption of a pure Fröhlich-type interaction.

[1] For an overview see J. Shah, *Ultrafast Spectroscopy of Semiconductors and Semiconductor Nanostructures*, (Springer, Berlin, 1996), and references therein.

[2] L. Schultheis, J. Kuhl, A. Honold, and C. W. Tu, Phys. Rev. Lett. **57**, 1635 (1986); **57**, 1797 (1986).

[3] P. C. Becker, H. L. Fragnito, C. H. Brito Cruz, R. L. Fork, J. E. Cunningham, J. E. Henry, and C. V. Shank, Phys. Rev. Lett. **61**, 1647 (1988).

[4] E. O. Göbel, K. Leo, T. C. Damen, J. Shah, S. Schmitt-Rink, W. Schäfer, J. F. Muller, and K. Köhler, Phys. Rev. Lett. **64**, 1801 (1990).

[5] A. Lohner, K. Rick, P. Leisching, A. Leitenstorfer, T. Elsaesser, T. Kuhn, F. Rossi, and W. Stolz, Phys. Rev. Lett. **71**, 77 (1993).

[6] M. U. Wehner, M. H. Ulm, D. S. Chemla, and M. Wegener, Phys. Rev. Lett. **80**, 1992 (1998).

[7] A. Leitenstorfer, C. Fürst, A. Laubereau, W. Kaiser, G. Tränkle, and G. Weimann, Phys. Rev. Lett. **76**, 1545 (1996).

[8] C. Fürst, A. Leitenstorfer, A. Laubereau, and R. Zimmermann, Phys. Rev. Lett. **78**, 3733 (1997).

[9] S. T. Cundiff, M. Koch, W. H. Knox, J. Shah, and W. Stolz, Phys. Rev. Lett. **77**, 1107 (1996).

[10] D. S. Kim *et al.*, Phys. Rev. Lett. **80**, 4803 (1998).

[11] A. Leitenstorfer, C. Fürst, and A. Laubereau, Opt. Lett. **20**, 916 (1995).

[12] C. Fürst, A. Leitenstorfer, and A. Laubereau, IEEE J. Sel. Top. Quantum Electron. **2**, 473 (1996).

[13] J.-P. Foing, D. Hulin, M. Joffre, M. K. Jackson, J.-L. Oudar, C. Tanguy, and M. Combescot, Phys. Rev. Lett. **68**, 110 (1992).

[14] J. A. Kash, J. C. Tsang, and J. M. Hvam, Phys. Rev. Lett. **54**, 2151 (1985).

[15] A. F. J. Levi, J. R. Hayes, P. M. Platzmann, and W. Wiegmann, Phys. Rev. Lett. **55**, 2071 (1985).

[16] H. Fröhlich, Proc. R. Soc. London, Ser. A **160**, 230 (1937).

[17] B. K. Ridley, *Quantum Processes in Semiconductors* (Clarendon Press, Oxford, 1993).

[18] L. Banyai, H. Haug, and P. Gartner, Eur. Phys. J. B **1**, 209 (1998).

[19] *Semiconductors–Basic Data*, edited by O. Madelung (Springer, Berlin, 1996).